

Spectroscopy Study of Synthetic Forsterite Obtained from Zeolite Precursors

KUI – 3/2008
Received October 2, 2006
Accepted February 28, 2007

C. Kosanović,^{a,*} N. Stubičar,^b N. Tomašić,^c M. Stubičar,^d
B. Subotić,^a A. Gajović,^a and L. Sekovanić^e

^a Ruđer Bošković Institute, Bijenička c. 54, 10 000 Zagreb, Croatia

^b Department of Chemistry, Faculty of Science, University of Zagreb, Horvatovac 102A, 10 000 Zagreb, Croatia

^c Institute of Mineralogy and Petrography, Faculty of Science, University of Zagreb, Horvatovac bb, 10 000 Zagreb, Croatia

^d Department of Physics, Faculty of Science, University of Zagreb, Bijenička c. 32, 10 002 Zagreb, Croatia

^e Geotechnical Faculty, Hallerova 7, 42 000 Varaždin, Croatia

Important ceramics materials are prepared from aluminosilicate based precursors using novel methods, offering at the same time a better control over many important properties. Forsterite, due to its good refractoriness with melting point at 2163 K, excellent electrical insulation properties even at high temperatures, low dielectric permittivity, thermal expansion and chemical stability, is a material of interest to engineers and designers especially as an active medium for tunable laser and is also a material of interest to SOFC (Solid oxide fuel cells) manufacturers.

The aim of this study is to investigate the synthesis of crystalline forsterite using different zeolite precursors previously activated by ball milling.

Synthetic forsterite was synthesized from different zeolite precursors and MgO combining high-energy ball milling and thermal treatment of the mixture under determined conditions of time and temperature for each operation. In this research are studied the solid-state phase transformations taking place at temperatures below 1273 K.

The obtained products were characterized using different spectroscopy techniques in comparison with surface analysis method and X-ray diffraction.

Key words: *Forsterite, ball milling, X-ray diffraction, FT-IR spectroscopy, Raman spectroscopy*

Introduction

Modern technologies constantly require new materials with special properties to achieve breathtaking innovations. This development focuses on the improvement of scientific and technological fabrication and working procedures. Among all these new materials, one group plays a very special role: glass-ceramic materials, because such types of material offer the possibility of combining the special properties of conventional sintered ceramics with the distinctive characteristics of glasses.¹ It is well known that glass-ceramics consist of at least one base glass phase and at least one crystalline phase, both coexisting and stable during use. Glass-ceramics are ceramic materials formed through the careful control of nucleation and crystallization processes in prepared amorphous (glass) materials.¹ In the design of glass-ceramics, the two most important factors are composition and microstructure. Today, there exist many available methods of powder formation. One of the most intriguing and widely used methods for processing powder materials

is by, no doubt, high-energy ball milling (HEBM). In the field of materials science, it has been recognized as a powerful tool in preparing novel materials. The HEBM processing of powders of elements, their mixtures or a master alloy usually induces formation of new non-equilibrium phase materials with functional characteristics, which very often could not be produced by other common processing techniques.

Zeolites are crystalline aluminosilicate materials with open framework structure.^{2–4} The chemical composition of zeolites may be generally represented by the formula: $\text{Me}_{2/z}\text{O} \cdot \text{Al}_2\text{O}_3 \cdot x\text{SiO}_2 \cdot y\text{H}_2\text{O}$, where Me is hydrated cation of ion charge number z which compensates the negative charge of the aluminosilicate framework and $x \geq 2$ is determined by the type of zeolite, while y , depending on the type of zeolite may vary from 0 – 10.^{2–5}

A very important property of zeolites is their ability to exchange the Metal cations located at specific sites in the channel-void system of zeolites with various cations from solutions.^{6–7}

It is well known that zeolites are metastable materials, which can be transformed to non-zeolite crystalline alumi-

* Corresponding author:
Cleo Kosanović, e-mail: cleo@irb.hr

nosilicates above a certain temperature.^{5, 8–13} Since many synthetic zeolites have composition close to those of aluminosilicate-based ceramics, their thermal treatment may result in the formation of appropriate ceramic materials.⁵ The advantage of zeolite precursors over conventional precursors is their property to sinter at much lower temperatures ($T < 1273$ K). Also, their uniform and narrow particle size distribution provides better control over the structure of the resulting ceramic phase.

Ball milling was used as an efficient method for the optimization of powder properties by means of combination and uttermost homogenization of the powder mass. High-energy ball milling of zeolites, as it is well-known from our previous studies, results in a decrease of crystallinity and the formation of X-ray amorphous phases (having the same chemical composition as the starting zeolites).^{14–16} Combining ball milling and thermal treatment of the starting mixture, it is possible to obtain nano-sized ceramic materials at much lower temperature than necessary for their synthesis without ball milling.

This study provides information on the microstructural evolution of the products obtained by HEBM and subsequent post-anneal processing of the mixture of NH_4 -ion exchanged zeolites and MgO powders as it is monitored by X-ray diffraction and other methods.

Experimental

Zeolite Linde 4A ($[\text{Na}_2\text{O} \cdot \text{Al}_2\text{O}_3 \cdot 1.98 \text{SiO}_2 \cdot 2.12 \text{H}_2\text{O}]$) or simply called zeolite A, synthesized in our laboratory, and synthetic mordenite ($[\text{Na}_2\text{O} \cdot \text{Al}_2\text{O}_3 \cdot 8.7 \text{SiO}_2 \cdot 7.24 \text{H}_2\text{O}]$), product of Union Carbide Corp., were used as starting materials. Ion exchange of the original Na^+ ions from the zeolite was carried out by an already described procedure.^{16–18} MgO was the product of Ventron with purity of 99.5%. The product was identified by X-ray diffraction analysis as periclase (MgO) [19; PDF 43-1022] and brucite ($\text{Mg}(\text{OH})_2$) [19; PDF 44-1482].

A mixture of NH_4 -exchanged zeolite A (NH_4A) and MgO (in a mass ratio of $\zeta = 1:0.15$) was mechanically treated in a high-energy planetary ball mill (Fritsch Pulverisette type 7). A certain mass (about $m = 2$ g) of the mixture was put in an agate vessel containing 10 agate balls ($d = 10$ mm) and 4 agate balls ($d = 12$ mm), and then milled for a predetermined time. The speed of mill rotation was $n = 3600 \text{ min}^{-1}$. The same procedure was repeated with the mixture of NH_4 -exchanged synthetic mordenite (NH_4SM) and MgO (in a mass ratio of $\zeta = 1:1$),

Thermal analysis of the sample obtained after 6 h of milling was performed using a Netzch STA 409 simultaneous thermal analysis apparatus under a constant airflow of rate $Q = 30 \text{ cm}^3 \text{ min}^{-1}$. Pt crucibles and alumina as a reference were used. The heating at the rate of temperature change was $\dot{T} = 10 \text{ K min}^{-1}$. The temperatures of the exothermic peaks in the DSC curves, as temperature of the phase transformations, were used as the experimental values for heating the samples.

Parts of the milled samples (1 gram of each) were heated isothermally at the temperature of $T = 1223$ K and $T = 1573$ K for 3 h.

Parts of the milled samples ($m = 1$ g of each) were pressed in a tablet (radius 6.5 mm) at $p = 7.540$ MPa. They were then heated at the temperature of $T = 1223$ K and $T = 1473$ K isothermally for 3 h.

Furthermore, the starting materials, the milled samples, the pressed samples and the subsequently post-annealed samples were characterized as follows:

Raman spectra were recorded using computerized DILOR Z24 triple monochromator with Coherent INNOVA 400 argon ion laser, operating at 514.5 nm line for excitation. An Anaspec's doublepass prism premonochromator was used to reduce parasite plasma lines. Laser power of $P = 150$ mW was applied. To reduce the heating of the sample during recording the Raman spectra, the shape of the incident laser beam was altered in line focus. The spectra were recorded in the region $15\text{--}1500 \text{ cm}^{-1}$ with $300 \mu\text{m}$ slit width.

The specific surface area of the crystals was determined by BET multiple method (Micromeritics Gemini) using nitrogen.

Infrared transmission spectra of the solid samples were obtained by the KBr wafer technique. The spectra were recorded using a FTIR spectrometer System 2000 FTIR (Perkin-Elmer) in the region of 400 to 4000 cm^{-1} (20 scans).

XRD patterns of the samples were obtained by means of Philips X'Pert PRO X-ray diffractometer using CuK radiation. Powder diffraction data were collected in the range from $4^\circ\text{--}63^\circ 2\theta$, with the steps of 0.02° (scan time 1474.5 s). The observed d -values and the relative intensities of the X-ray diffraction lines, as well as the cell parameters were compared with the literature values reported (PDF-s).¹⁹

Results and discussion

The Raman spectra of olivine, to which forsterite belongs, can be divided into 3 regions: $<400 \text{ cm}^{-1}$, $400\text{--}800 \text{ cm}^{-1}$, and $800\text{--}1100 \text{ cm}^{-1}$.²⁰ Peaks between 800 and 1100 cm^{-1} are attributed to SiO_4 internal stretching vibrational modes. The dominant features obtained in that region were a doublet with peaks at 827 and 856 cm^{-1} (see Fig. 1 and Fig. 2) whose relative heights are the function of crystal orientation.

These peaks result from the coupled symmetric and asymmetric vibrations of SiO_4 tetrahedra. Peaks in the $400\text{--}800 \text{ cm}^{-1}$ region are mainly from SiO_4 internal bending vibrational modes.

Peaks below 400 cm^{-1} are mostly contributed by lattice modes: rotations and translations of SiO_4 units and translations of octahedral coordinated cations in the crystal lattice.^{21–22} The Raman spectra of the sample obtained after heating of NH_4A and MgO previously ballmilled gave no information because of the fluorescence of Al in the sample. Therefore, the product was characterized by other methods such as X-ray diffraction method and FTIR spectroscopy and the results are listed hereafter. The Raman spectra of the sample obtained after heating the mixture of NH_4SM and MgO contained all characteristic peak assignments for forsterite (denoted in Fig. 2) in comparison with the table data given by C. C. Lin.²³

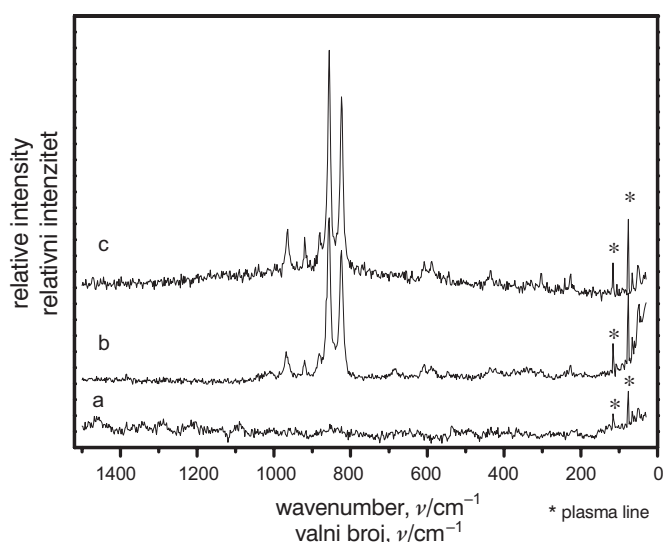


Fig. 1 – Raman spectra of the mixture of NH_4A and MgO ball milled for 10 h (a), and heated at 1223 K (b) and 1573 K (c) for 3 h
Slika 1 – Ramanski spektar smjese NH_4A i MgO , mljevene kugličnim mlinom 10 h (a) i grijane 3 h pri 1223 K (b) i 1573 K (c)

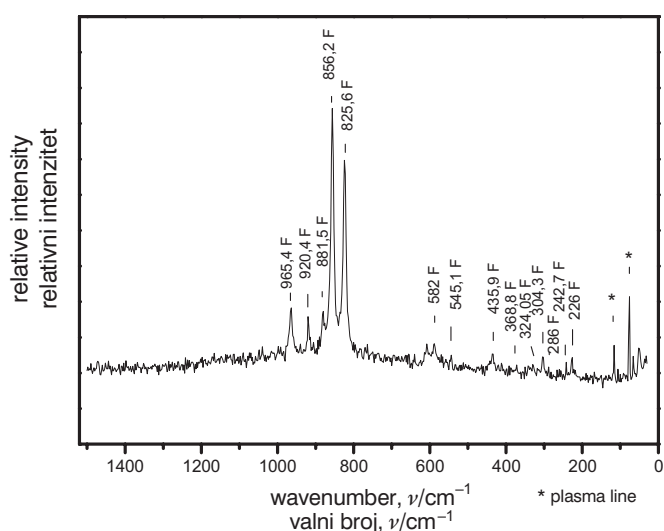


Fig. 2 – Raman spectra of the mixture of NH_4SM and MgO ball milled for 10 h and heated at 1573 K for 3 h, with the bands of forsterite marked (F – forsterite)

Slika 2 – Ramanski spektar smjese NH_4SM i MgO , mljevene kugličnim mlinom 10 h i grijane 3 h pri 1573 K s označenim vrpca-ma forsterita (F – forsterit)

The FTIR spectra for the sample obtained after ball milling and heating of the mixture of the NH_4A and MgO in the interval from $T = 1123$ – 1573 K are presented in Fig. 3.

Most of the marked bands in the spectrum (a) such as 463, 526, 616, 1003 cm^{-1} belonged to a forsterite phase^{22, 24} since the very broad band at high frequency in the range 3440–3600 cm^{-1} belonged to OH-stretching. This indicated that either H_2O or weakly bonded OH or both, were present.

All other bands belong to another phase that was characterized by the X-ray diffraction (Fig. 5). At the temperature

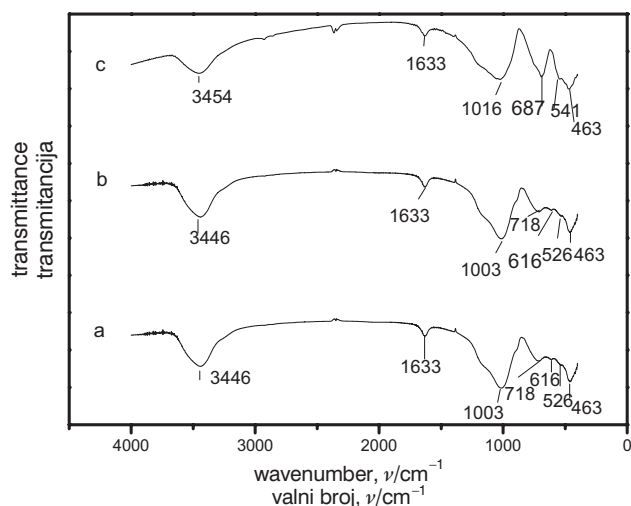


Fig. 3 – Infrared transmission spectra of the mixture of NH_4A , and MgO ball milled for 10 h and heated at 1123 K (a), 1223 K (b) and 1573 K (c) for 3 h

Slika 3 – Infracrveni transmisijski spektar smjese NH_4A i MgO , mljevene kugličnim mlinom 10 h i grijane 3 h pri 1123 K (a), 1223 K (b) i 1573 K (c)

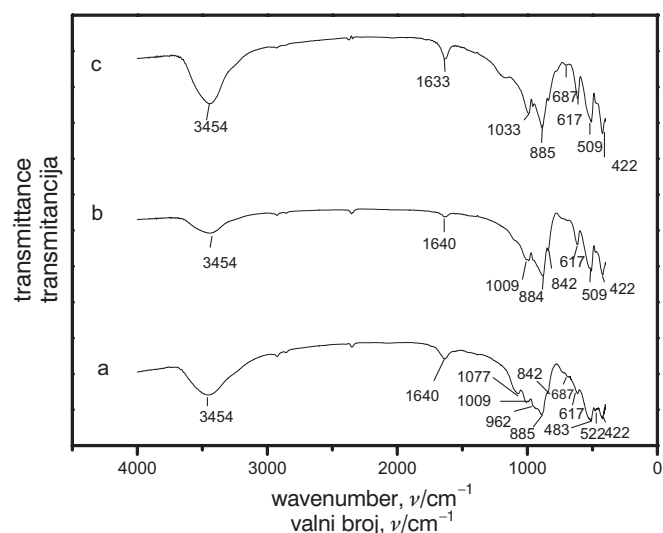


Fig. 4 – Infrared transmission spectra of the mixture of NH_4SM and MgO after 10 h of ball milling heated at 1123 K (a), 1223 K (b) and 1573 K (c) for 3 h

Slika 4 – Infracrveni transmisijski spektar smjese NH_4SM i MgO , mljevene kugličnim mlinom 10 h i grijane 3 h pri 1123 K (a), 1223 K (b) i 1573 K (c)

of 1123 K (Fig. 5a) two crystalline phases coexisted, crystalline forsterite (Mg_2SiO_4 , PDF 34–0189)¹⁹ and a spinel (MgAl_2O_4 , PDF 21–1152).¹⁸ By further heating to 1223 K (Fig. 5b) the sample was more crystalline but the phases remained the same.

By heating the sample at a temperature over 1273 K (Fig. 5c) a small amount of enstatite (MgSiO_3 , PDF 19–0605)¹⁹ appeared along with the forsterite and the spinel phase.

In order to achieve a higher ratio of forsterite phase in comparison to the other forming phases, it was necessary to use a starting mixture with higher $\zeta_{\text{SiO}_2/\text{Al}_2\text{O}_3}$ mass ratio, like in synthetic mordenite.

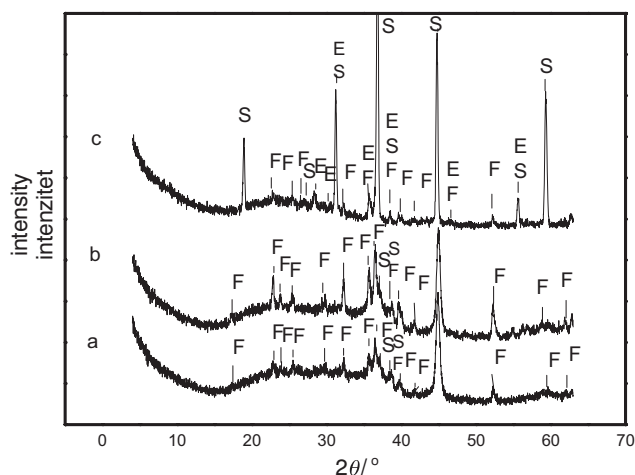


Fig. 5 – X-ray diffractograms of the mixture of NH_4A and MgO after 10 h of ball milling heated at 1123 K (a), 1223 K (b) and 1573 K (c) for 3 h (F – forsterite, E – enstatite, S – spinel)

Slika 5 – Rendgenogrami smjese NH_4A i MgO , mljevene kugličnim mlinom 10 h i grijane 3 h pri 1123 K (a), 1223 K (b) i 1573 K (c) (F – forsterit, E – enstatit, S – spinel)

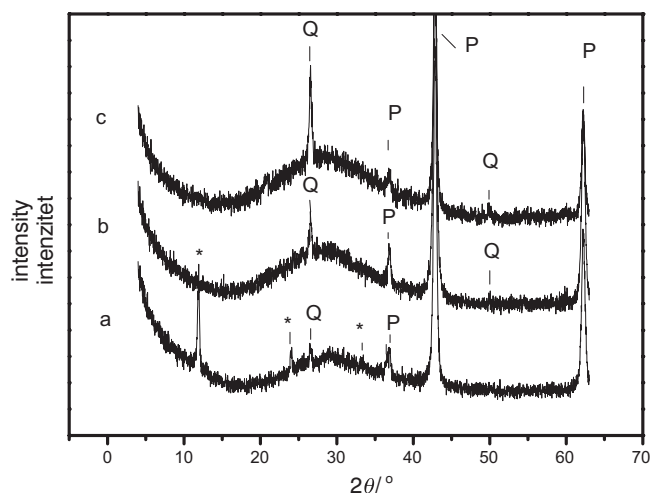


Fig. 6 – X-ray diffractograms of the mixture of NH_4SM and MgO after 10 h (a), 13 h (b), and 24 h (c) of ball milling (The marks Q, P and * correspond to quartz, periclase and the holder lines)

Slika 6 – Rendgenogrami smjese NH_4SM i MgO , mljevene kugličnim mlinom 10 h (a), 13 h (b), i 24 h (c) (Oznake Q, P i * odnose se na kvarc, periklas i linije nosača)

Also, the sufficient milling time was estimated to be about 10 h (Fig. 6). The diffraction pattern of the mixture showed that the zeolite phase was completely amorphous, and the MgO particle size was decreased (Fig. 6a). Continuing the ball milling for 13 h (Fig. 6b) the amorphous SiO_2 started to crystallize to quartz and the quantity increased with further milling (Fig. 6c).

The same conclusion could be drawn by analyzing the changes obtained by the BET measurements (Table 1). At the beginning of milling, the surface area increased due to the amorphization of the mixture.

After a few hours, the formation of crystalline SiO_2 caused the decrease of the specific surface. An analogue behavior was observed when studying the evolution of the phase of the mixture NH_4SM and MgO during milling (Table 2).

Tablica 1 – Changes in the specific surface area of mixture NH_4A and MgO during ball milling and change in the specific area after heating of the sample milled for 5 h at 1573 K for 1 h

Table 1 – Promjene specifične površine smjese NH_4A i MgO u ovisnosti o vremenu mljevenja kugličnim mlinom i promjene specifične površine uzorka mljevenog 5 h i grijanog 1 h pri 1573 K

Time of milling Vrijeme mljevenja t/h	Multipoint specific surface area Specifična površina smjese $\text{a/m}^2\text{g}^{-1}$	Single point specific surface area Specifična površina uzorka $\text{a/m}^2\text{g}^{-1}$
0.167	11.934	11.467
1	15.480	14.840
3	15.187	14.508
5	11.824	11.297
20	10.609	10.029
heated at 1573 K for 1 h – grijano 1 h pri 1573 K		
	<0.3	<0.3

Tablica 2 – Changes in the specific surface area of mixture NH_4SM and MgO during the ball milling and the change in the specific area after heating of the sample milled for 10 h at 1573 K for 1 h

Table 2 – Promjene specifične površine smjese NH_4SM i MgO u ovisnosti o vremenu mljevenja kugličnim mlinom i promjene specifične površine uzorka mljevenog 10 h i grijanog 1 h pri 1573 K

Time of milling t/h Vrijeme mljevenja t/h	Multipoint specific surface area Specifična površina smjese $\text{a/m}^2\text{g}^{-1}$	Single point specific surface area Specifična površina uzorka $\text{a/m}^2\text{g}^{-1}$
0.167	21.250	20.286
1	16.707	16.013
3	10.837	10.325
10	7.831	7.039
24	6.766	6.384
heated at 1573 K for 1 h – grijano 1h pri 1573 K		
	<0.3	<0.3

Again, studying the IR-spectra (Fig. 4) and the X-ray diffraction patterns (Fig. 7) obtained for the NH_4SM and MgO mixture in the interval from $T = 1123$ – 1573 K, we noticed that at the temperature of $T = 1123$ K (Fig. 7a) a major amount of forsterite phase (Mg_2SiO_4 , PDF 34–0189)¹⁹ and minor amounts of enstatite (MgSiO_3 , PDF 19–0605)¹⁹ co-existed. The dominating crystalline phase at the temperature $T = 1223$ K (Fig. 7b), was crystalline forsterite (Mg_2SiO_4 , PDF 34–0189)¹⁹ while at higher temperatures (Fig. 7c) cordierite ($\text{Mg}_2\text{Al}_4\text{Si}_5\text{O}_{18}$, PDF 13–0294)¹⁹ appeared as a minor phase along with the forsterite phase (Mg_2SiO_4 , PDF 34–0189).¹⁹

After treating under pressure of $p = 7.540$ MPa and heating at the temperature of $T = 1223$ K and 1473 K respectively, both samples (mixture: NH_4A and MgO , see Fig. 8 and mixture: NH_4SM and MgO , see Fig. 9) transformed into forsterite as the main phase, but the obtained minor phases changed.

As it was characterized by diffraction analysis, a small amount of the mixture: NH_4A and MgO was transformed

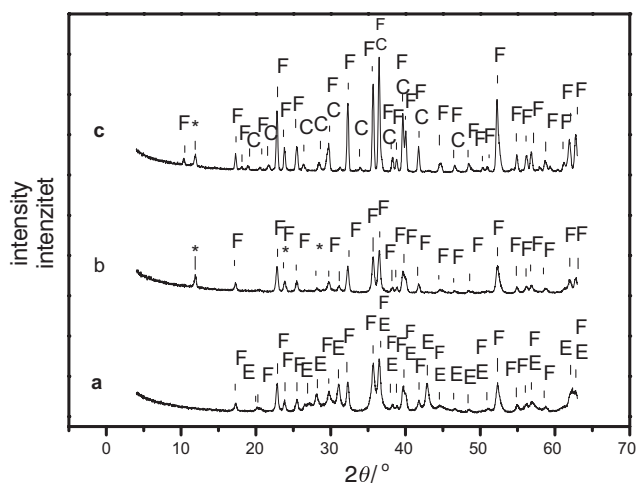


Fig. 7 – X-ray diffractograms of the mixture of NH_4SM and MgO after 10 h of ball milling heated at 1123 K (a), 1223 K (b) and 1573 K (c) for 3 h (F – forsterite, E – enstatite, C – cordierite, * corresponds to the holder lines)

Slika 7 – Rendgenogrami smjese NH_4SM i MgO , mljevene kugličnim mlinom 10 h i grijane 3 h pri 1123 K (a), 1223 K (b) i 1573 K (c) (F – forsterit, E – enstatit, C – kordijerit, * odnosi se na linije nosača)

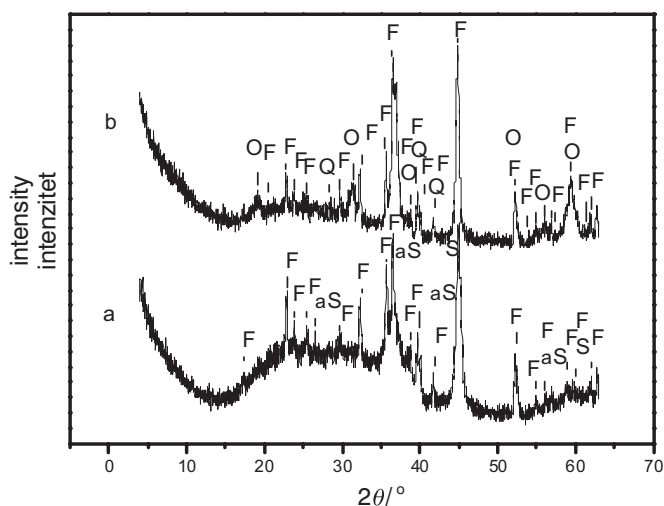


Fig. 8 – X-ray diffractograms of the mixture of NH_4A and MgO after 10 h of ball milling, pressed at 7.540 MPa, and then heated at 1223 K (a), and 1473 K (b) for 3 h (F – forsterite, S – spinel, Q – quartz, αS – silicon oxide and magnesium dialuminium oxide)

Slika 8 – Rendgenogrami smjese NH_4A i MgO , mljevene kugličnim mlinom 10 h, prešane u tablete pod tlakom 7,540 MPa i grijane 3 h pri 1223 K (a) i 1473 K (b) (F – forsterit, S – spinel, Q – kvarc, αS – silicijev oksid i O – magnezijev dialuminijev oksid)

also to SiO_2 as α -silicon oxide (SiO_2 , PDF 01–089-8937) at $T = 1223$ K and quartz (SiO_2 , PDF 01–070-3317) at $T = 1473$ K and the mixture: NH_4SM and MgO , as a minor phase at $T = 1223$ K formed quartz (SiO_2 , PDF 01–070-2517) and at higher temperature, as a minor phase formed only magnesium aluminium catena aluminosilicate ($(\text{Mg}_{0.956}\text{Al}_{0.044})(\text{Al}_{0.044}\text{Si}_{0.956}\text{O}_3)$, PDF 01-076-2428).

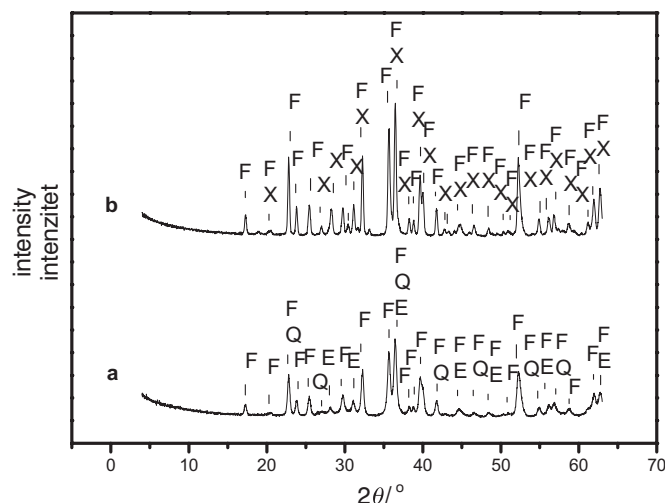


Fig. 9 – X-ray diffractograms of the mixture of NH_4SM and MgO after 10 h of ball milling, pressed at 7.540 MPa and then heated at 1223 K (a), and 1473 K (b) for 3 h (F – forsterite, E – enstatite, S – spinel, Q – quartz and X – magnesium aluminium catena-aluminosilicate)

Slika 9 – Rendgenogrami smjese NH_4A i MgO , mljevene kugličnim mlinom 10 h, prešane u tablete pod tlakom 7,540 MPa i grijane 3 h pri 1223 K (a) i 1473 K (b) (F – forsterit, S – spinel, Q – kvarc, X – magnezijev aluminijev katena-alumosilikat)

Conclusion

The results of this paper offer an attractive possibility for the synthesis of glass-ceramics materials or pure crystalline forsterite powders if a proper amount of NH_4 -ion exchanged zeolites and MgO powder are used. Specifically, a higher mass fraction of forsterite in the product may obtain using different ratios of MgO and zeolite precursors with higher ratio of $\text{SiO}_2/\text{Al}_2\text{O}_3$ in their composition.

Synthesis of forsterite using zeolite precursors and MgO is confirmed by Infrared and Raman spectroscopy as well by X-ray diffraction method.

The additional treatment with pressure does not effect to the formation of the main product but changes composition of the minor phases obtained. Higher temperature was used in order to produce better crystalline product.

Formation of the forsterite-based glass-ceramics revealed in this study might be explained by using the equilibrium phase diagram established for the Al_2O_3 - MgO - SiO_2 system.

ACKNOWLEDGMENT

The authors wish to thank the Ministry of Science, Education and Sport of the Republic of Croatia for the financial support, and Dr. Jasmina Kontrec for the BET measurements.

List of symbols**Popis simbola**

Me	– metal cation – metalni kation
z	– valence of cation – valencija kationa
x, y	– molar coefficient – molarni koeficijent
HEBM	– high energy ball milling
F	– forsterite – forsterit
E	– enstatite – enstatit
S	– spinel – spinel
Q	– quartz – kvarc
P	– periclase – periklas
*	– holder line – linija nosača
C	– cordierite – kordijerit
α S	– silicon oxide – silicijev dioksid
O	– magnesium dialuminium oxide – magnezijev dialuminijev oksid
X	– magnesium aluminium catena-aluminosilicate – magnezijev aluminijev katena-alumosilikat
a	– specific surface area, $\text{m}^2 \text{g}^{-1}$ – specifična površina, $\text{m}^2 \text{g}^{-1}$
d	– diameter, mm – promjer, mm
m	– mass, g – masa, g
n	– rotation speed, min^{-1} – brzina vrtnje, min^{-1}
P	– power, mW – snaga, mW
p	– pressure, MPa – tlak, MPa
Q	– volume flow rate, $\text{cm}^3 \text{min}^{-1}$ – obujmni protok, $\text{cm}^3 \text{min}^{-1}$
T	– temperature, K – temperatura, K

\dot{T}	– rate of temperature change, K min^{-1} – brzina temperaturne promjene, K min^{-1}
ζ	– mass ratio, m_1/m_2 – maseni omjer, m_1/m_2
Θ	– Bragg angle, $^\circ$ – Braggov kut, $^\circ$
ν	– wavenumber, cm^{-1} – valni broj, cm^{-1}

References

1. Glass-Ceramic Technology, W. Höland, G. Beall, The American Ceramic Society, Westerville, 2002.
2. D. W. Breck, *J. Chem. Educ.* **41** (1964) 678.
3. Principles of Synthesis and Identification, R. Szostak in Molecular Sieves; edited by Van Nostrand Reinhold, New York, 1989.
4. Synthesis, Characterization and Use of Zeolitic Microporous Materials, J. B. Nagy, P. Bodart, I. Hannus, I. Kiricsi; edited by Deca Gen, Szeged, 1998.
5. M. A. Subramanian, D. R. Corbin, U. Chowdhry, *Bull. Mater. Sci.* **16** (1993) 665.
6. H. S. Sherry, *Adv. Chem. Ser.* **101** (1971) 350.
7. R. M. Barrer, J. Klinowski, *Phil. Trans.* **285** (1977) 637.
8. M. Holioka, *J. At. Energ. Soc. Jpn.* **11** (1969) 406.
9. H. Mimura, T. Kanno, *Sci. Rep. RITU* **29A** (1980) 102.
10. R. L. Bedard, R. W. Broach, E. M. Flanigen, in: Proc. Symp. Better Ceramics Through Chemistry V; edited by M. J. Hampden-Smith, W. G. Klemperer, C. J. Brinker, Materials Research Society, Pittsburgh, PA, 1992.
11. B. Hoghooghi, J. McKittrick, C. Butler, P. Desch, *J. Non-Cryst. Solids* **170** (1994) 303.
12. C. Kosanović, B. Subotić, I. Šmit, *Thermochim. Acta* **317** (1998) 25.
13. G. Dell'Agli, C. Ferone, M. C. Mascolo, M. Pansini, *Solid State Ionics* **127** (2000) 309.
14. C. Kosanović, J. Bronić, B. Subotić, I. Šmit, M. Stubičar, A. Tonejc, T. Yamamoto, *Zeolites* **13** (1993) 261.
15. C. Kosanović, J. Bronić, A. Čižmek, B. Subotić, I. Šmit, M. Stubičar, A. Tonejc, *Zeolites* **15** (1995) 247.
16. C. Kosanović, B. Subotić, I. Šmit, *Croat. Chem. Acta* **74** (2001) 195.
17. C. Kosanović, A. Čižmek, B. Subotić, I. Šmit, M. Stubičar, A. Tonejc, *Zeolites* **15** (1995) 632.
18. C. Kosanović, B. Subotić, *Micropor. Mater.* **12** (1997) 261.
19. JCPDS International Centre for Diffraction Data, Swarthmore, PA, 1996.
20. H. Takei, *J. Crystal Growth* **43** (1978) 463.
21. A. Chopelas, *Am. Min.* **76** (1991) 1101.
22. T. P. Mernacgh, L.-G. Liu, *The Canadian Mineralogist* **36** (1998) 1217.
23. C. C. Lin, *Phys. Chem. Minerals* **28** (2001) 249.
24. D. G. Park, J. C. Duchamp, T. M. Duncan, J. M. Burlitch, *Chem. Mater.* **6** (1994) 1990.

SAŽETAK

Spektroskopski studij sintetskog forsterita dobivenog iz zeolitnih prekursora

C. Kosanović,^a N. Stubičar,^b N. Tomašić,^c M. Stubičar,^d B. Subotić,^a A. Gajović^a i L. Sekovanić^e

Važni keramički materijali pripremljeni su iz alumosilikatnih prekursora, pri čemu su primijenjene novije metode, koje istodobno daju mogućnost intervencije u procese nastajanja i kontrolu nad mnogim svojstvima. Forsterit je silikatni materijal posebno interesantan inženjerima i konstruktorima procesne opreme, osobito u laserskoj tehnici i području gorivih čvrstih oksidnih ćelija (SOFC), zbog svoje kemijske stabilnosti, dobrih vatrostalnih karakteristika, tališta od 2163 K, izvrsnih električkih izolacijskih svojstava, male električne permitivnosti i slabog termičkog širenja.

Cilj ovog rada je istraživanje na području sinteze kristalnog forsterita uz upotrebu različitih zeolitnih prekursora koji su prethodno aktivirani mljevenjem kugličnim mlinom. Sintetski forsterit dobio je iz smjese MgO i različitih zeolitnih prekursora, kombinirajući visoko energijsko mljevenje i termičku obradu u kontroliranim vremenskim i temperaturnim uvjetima. U ovom istraživanju studirane su fazne transformacije čvrstog stanja koje se odvijaju na temperaturama ispod 1273 K.

Dobiveni proizvod je opisan pomoću različitih spektroskopskih tehnika, analizom specifične površine i rendgenskom difrakcijom.

^a Institut Ruđer Bošković, Bijenička c. 54,
10 000 Zagreb, Hrvatska

Prispjelo 2. listopada 2006.
Prihvaćeno 28. veljače 2007.

^b Prirodoslovno-matematički fakultet, Kemijski odsjek,
Sveučilište u Zagrebu, Horvatovac 102A, 10 000 Zagreb, Hrvatska

^c Prirodoslovno-matematički fakultet, Geološki odsjek,
Sveučilište u Zagrebu, Horvatovac bb, 10 000 Zagreb, Hrvatska

^d Prirodoslovno-matematički fakultet, Fizički odsjek,
Sveučilište u Zagrebu, Bijenička c. 32, 10 000 Zagreb, Hrvatska

^e Geotehnički fakultet, Hallerova 7, 42 000 Varaždin, Hrvatska